# Isothermal crystallization kinetics of poly(ether ketone ketone) and its carbon-fibre-reinforced composites

**Benjamin S. Hsiao*, Ike Y. Chang and Bryan B. Sauer†**
*Fibers and †Central Research and Development, Experimental Station, E.I. Du Pont de Nemours Co & Inc., Wilmington, DE 19880, USA*
*(Received 14 June 1990; accepted 3 August 1990)*

Isothermal crystallization kinetics of poly(ether ketone ketone) (PEKK) and its carbon-fibre-reinforced composites was analysed by using a phenomenological two-stage crystallization kinetics model modified from the Avrami equation. We have determined a different Avrami exponent for each crystallization stage from differential scanning calorimetry isothermal measurements. In the primary crystallization stage, the nucleation growth is assumed to be three-dimensional, sporadic and with an Avrami exponent of 4; whereas in the secondary stage, it is assumed to be two-dimensional or diffusion-controlled, with an Avrami exponent of 2. This model gives a considerably better fit than the unmodified Avrami equation and the two-stage Velisaris–Seferis model. The estimated final volume fraction crystallinity of the primary crystallization is approximately 60% over the temperature range of 298–314°C. Cold crystallization produces a higher value of the primary volume crystallinity ranging from 70% to 100% over the temperature range of 221–200°C. The presence of fibre in the composite does not change the relative primary volume crystallinity nor does it affect rate constants of both stages. The effect of fibre on the total crystallization rate of PEKK in the composite is also small.

**(Keywords: poly(ether ketone ketone); composites; isothermal crystallization kinetics; modified two-stage Avrami model)**

## INTRODUCTION

Poly(aryl ether ketones) are used as matrix resins in advanced high-performance composites because of their high temperature stability, excellent environmental performance and superior mechanical properties. Their polymer derivatives include poly(ether ether ketone) (PEEK), poly(ether ketone) (PEK), poly(ether ketone ether ketone ketone) (PEKEKK) and poly(ether ketone ketone) (PEKK). These materials differ from each other in the ratio of keto/ether linkages and the ratio of *para/meta* phenyl isomers[1]. PEEK, PEK and PEKEKK are strictly *para*-linked aromatic polymers, whereas PEKK consists of *para* and *meta* isomers. From the molecular standpoint, a keto linkage is stiffer than an ether linkage. Thus, the increase in keto linkages inevitably increases the glass transition temperature, melting temperature and melt viscosity. For example, PEEK has a $T_g$ of 144°C and a $T_m$ of 334 to 343°C; PEK has a $T_g$ of 154°C and a $T_m$ of 367°C; PEKEKK has a $T_g$ of 173°C and a $T_m$ of 370°C[2–4]. In principle, all *para*-linked PEKK will have a higher glass temperature and melting temperature than PEEK, PEK and PEKEKK. Addition of the *meta* isomers in PEKK significantly reduces its $T_m$ and melt viscosity, while a high $T_g$ is retained; PEKK has a $T_g$ of 156°C and a $T_m$ of 330 to 339°C[5,6]. The crystallization kinetics of different poly(aryl ether ketones) is also expected to be different, because of their different molecular mobilities.

Several laboratories have studied the isothermal crystallization kinetics of PEEK and its composites[7–10]. They often observed that experimental isotherms deviate markedly from the theoretical Avrami model. An Avrami equation can partially describe the isotherm only at the early stage of crystallization, which is referred to as the primary crystallization stage. At this stage, the spherulite growth rate is approximately constant[11], and the Avrami exponent is generally between 3 and 4[8,9], though a lower value of 2.5 has also been reported[7]. As spherulite impingement occurs, departure from the simple Avrami relationship is usually observed and the crystallization rate decreases significantly. This process is attributed to the secondary crystallization within the spherulite. This later stage can also be expressed by an Avrami equation with a lower value of the exponent, indicating that the crystal growth becomes lower-dimensional or more diffusion-controlled[12]. The Avrami exponent of the secondary crystallization stage for PEEK is 2.5 to 1.5[7,8].

Attempts have been made to incorporate both primary and secondary crystallization processes into the crystallization kinetics modelling of polymers[7,13,14]. Perhaps the most logical approach was proposed by Hillier in 1965[13]. In this approach, the primary crystallization is expressed by an Avrami equation:

$$X_p(t) = X_p^0[1 - \exp(-K_p t^n)] \quad (1)$$

where $X_p(t)$ is the relative volume fraction crystallinity at time $t$, $X_p^0$ is the relative volume fraction crystallinity of the primary stage at infinite time (equal to or less than 1), $K_p$ is the rate constant depending upon nucleation and growth rates (or temperature) and $n$ is the Avrami exponent depending on the shape of the growing crystalline body. The secondary crystallization process, which occurs at time $\tau$, can also be expressed by a simple Avrami equation. The additional crystallinity at time $t$

* To whom correspondence should be addressed

0032-3861/91/152799-07
© 1991 Butterworth-Heinemann Ltd.

is thus given by:

$$X_s(t-\tau)=X_s^0\{1-\exp[-K_s(t-\tau)^m]\} \quad (2)$$

where $X_s^0$ is the relative volume fraction crystallinity of secondary crystallization at infinite time, $K_s$ is the rate constant and $m$ is the Avrami exponent of this stage. The total volume fraction crystallinity $X_c(t)$ is the sum of the above two crystallinities:

$$X_c(t)=X_p(t)+\int_t^0 [X_p(\tau)/X_p^0]\{\partial[X_s(t-\tau)]/\partial\tau\}\,d\tau \quad (3)$$

From equations (1), (2) and (3):

$$X_c(t)=X_p^0[1-\exp(-K_p t^n)] + X_s^0 K_s m \int_t^0 [1-\exp(-K_p\tau^n)](t-\tau)^{m-1} \times\{1-\exp[-K_s(t-\tau)^m]\}\,d\tau \quad (4)$$

where $X_p^0+X_s^0=1$, indicating that the total relative volume fraction crystallinity at infinite time is unity. Hillier assumed that the primary Avrami exponent $n$ was 3 or 4, and the secondary crystallization was a first-order process with the exponent $m$ equal to unity. He used this model to fit the experimental data from polyethylene, poly(ethylene oxide) and poly(decamethylene terephthalate) and concluded that the fit was significantly better than the unmodified Avrami equation.

A different two-stage crystallization model was also utilized by Velisaris and Seferis[7] to analyse the crystallization kinetics of PEEK and its AS-4 carbon-fibre-reinforced composite (APC-2). It was based on a parallel or a series combination of two independent Avrami equations. Each equation described a different crystallization stage. This model also provides a satisfactory numerical fit to the experimental data, particularly in the case of the parallel one. They reported that a significant difference in crystallization kinetics was observed between PEEK (450G resin) and the APC-2 composite.

In this work, we use the generalized Hillier approach to analyse the crystallization kinetics of PEKK and its carbon-fibre-reinforced composites, and compare it with the two-stage Velisaris–Seferis model. Using this approach, we have determined the volume fraction crystallinity and the temperature-dependent rate constants, for the primary and the secondary crystallization stages, respectively.

## EXPERIMENTAL

The PEKK resin used in this study was made by Du Pont with the following chemical structure[5,6]:

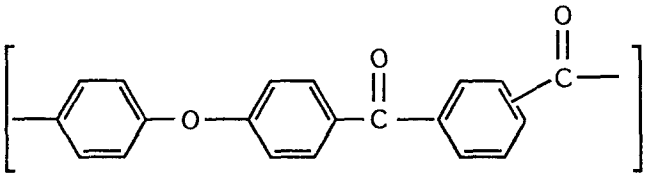

It has an inherent viscosity of approximately 0.7 as determined at 25°C in a solution of 0.1 g polymer per 100 ml sulphuric acid (96.3%). Its $M_n$ is about 9000 and $M_w$ is about 30000, measured by a g.p.c. analysis (calibrated by polystyrene standards). An AS-4 carbon-fibre-reinforced PEKK (the same resin) prepreg made from a melt impregnation process was also used to study the crystallization kinetics of the composite. The prepreg has a fibre content of approximately 60% by volume.

The isothermal crystallization analysis was carried out in a Perkin–Elmer DSC 7 station. In all cases, specimens were initially equilibrated at 380°C for 5–10 min. This temperature is above its equilibrium melting temperature, which is about 354°C[15]. Two separate techniques were used to study d.s.c. isotherms. The first method employed the cooling of the polymer melt at a rate of 320°C min$^{-1}$ to a desired isothermal crystallization temperature (between 270 and 310°C) and measured the melt crystallization exotherms. The second technique involved the quenching of the melt with liquid nitrogen to room temperature, then subsequent heating to the isothermal temperature (190 to 230°C) at a rate of 320°C min$^{-1}$ to measure cold crystallization. The liquid nitrogen quenching process was used to eliminate possible crystallinity developed near the maximum crystallization temperature.

D.s.c. isotherms were analysed by using the proposed model program in a Cray X-MP computer station. This program was developed in FORTRAN language utilizing a NAG (Numerical Algorithms Group, NAG Inc., Illinois) software package for numerical subroutines. The proposed model (equation (4)) contains three parameters: $X_p^0$, $K_p$ and $K_s$. The best fit was determined by minimization of the sum of the squares of the differences between the model and the data using the initial guess values ($X_p^0$, $K_p$ and $K_s$) estimated from an unmodified Avrami equation. A typical CPU time for a single fit using the Cray computer is about 20–50 s.

## RESULTS AND DISCUSSION

A typical d.s.c. isotherm of a supercooled PEKK specimen from melt crystallization is illustrated in *Figure 1*. The area within this curve represents a normalized crystalline content of unity, and the relative volume fraction of crystallinity at time $t$, $X_c(t)$, can be determined by dividing the partial area by the overall area. In *Figure 1*, the exothermic curve is highly asymmetric. At short times (less than 18 s), the heat flow signals are unstable as a result of d.s.c. mode switching from cooling to isothermal (or heating to isothermal) operations. Therefore, if the crystallization process is fast,

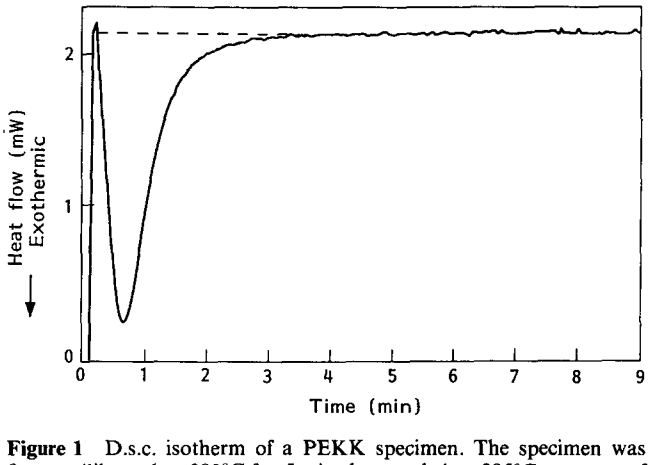


**Figure 1** D.s.c. isotherm of a PEKK specimen. The specimen was first equilibrated at 380°C for 5 min then cooled to 295°C at a rate of 320°C min$^{-1}$ for the isothermal measurement

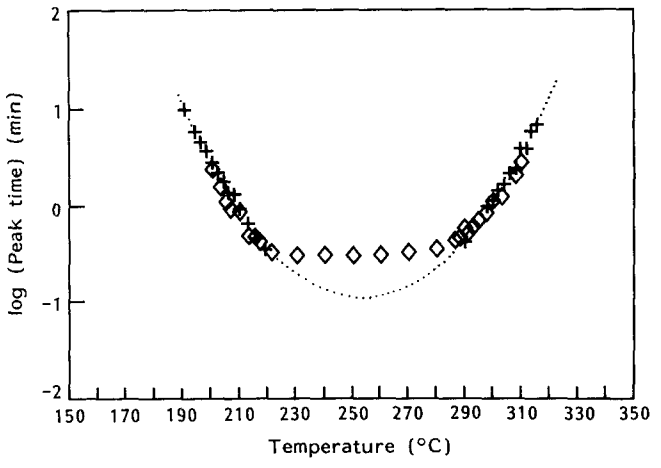


**Figure 2** Crystallization peak time vs. temperature for PEKK resin and its AS-4 carbon-fibre-reinforced composite. The dotted curve represents the fit from a second-order polynomial equation. ◇, PEKK; +, AS-4/PEKK

the initial signals may be truncated by instrumental fluctuations, and the measured area may no longer represent the total enthalpy change of crystallization.

The crystallization half-time $t_{1/2}$, defined as the time at which the relative crystallization content is 50%, *versus* temperature diagram is a useful tool to characterize the crystallization kinetics of polymers. For polymers having a fast crystallization rate such as PEKK, the estimated $t_{1/2}$ can involve a great degree of inaccuracy. Therefore, it is reasonable to substitute $t_{1/2}$ with the peak time to study the crystallization kinetics. This peak time represents the time that maximum heat flow is detected, which is less sensitive to the initial instrumental fluctuations. The physical meaning of this peak time will be discussed later.

The crystallization peak time (on logarithmic scale) *versus* temperature plots of the PEKK neat resin and its carbon-fibre-reinforced composite are shown in *Figure 2*. Data points above 260°C were directly obtained from quenched melts (melt crystallization), whereas data points below 260°C were measured from annealing of amorphous solid specimens (cold crystallization). The results are quite symmetrical. In *Figure 2*, measured peak times from 220 to 280°C are relatively constant (0.3–0.35 min). These values are very close to the d.s.c. detection limit and are inaccurate. We must extrapolate the minimum crystallization peak time from the high- and low-temperature data. Such data points are numerically fitted with a second-order polynomial equation as shown by the dotted curve in *Figure 2*. The extrapolated minimum peak time is about 0.13 min at 255°C, which is higher than that of PEEK (0.07 min at 230°C)[16].

In *Figure 2*, we observed little difference in the crystallization kinetics between the PEKK neat resin and its carbon-fibre composite. Since the carbon fibre has a much higher value of thermal conductivity than PEKK, the similar crystallization kinetics implies that the specimen temperature in the d.s.c. isothermal study was near equilibrium. The low thermal conductivity of PEKK resins did not hinder the heat transfer in the measurement. This observation is different from the case of poly(phenylene sulphide) (PPS). In this case, the crystallization rate was significantly increased by adding carbon or aramid fibre to PPS[17]. The difference between the case of PEKK and PPS may be explained as follows. The nucleating ability of PEKK is sufficiently high so the addition of carbon fibre does not further increase its nucleating power. In contrast, PPS nucleates much more slowly so that the fibre may become an effective nucleating agent. The phenomenon of fibre-surface-induced nucleation in high-performance matrix resins (PEKK, PEEK and PPS) has been discussed recently by Hsiao *et al.*[18,19]. They concluded that the similar unit cell in the aramid fibre and the graphite edge plane in the carbon fibre are all possible sources to induce the nucleation in these polymers. In the case of PEEK, the effect of fibre on its crystallization kinetics may be similar to that in PEKK, because of its intrinsically rapid crystallizing ability. This argument is different from Velisaris *et al.*'s conclusion that the carbon fibre has a significant effect on crystallization kinetics of PEEK, based on pair comparison between PEEK (450G resin) and APC-2 composite. It is known that the matrix resin used for APC-2 composite is similar to PEEK (150G), which has a lower molecular weight than that of PEEK (450G). Thus, it is difficult to conclude whether the observed difference in crystallization kinetics is due to the different molecular weight in PEEK resins, or to the presence of carbon fibres or possibly the addition of a nucleating agent in APC-2.

Isothermal crystallization results of PEKK are summarized in *Figures 3* and *4*, where $\ln\{-\ln[1-X_c(t)]\}$ vs. $\ln(t)$ at different temperatures are plotted. *Figure 3* is constructed from the data of melt crystallization, and *Figure 4* is from that of cold crystallization. In both cases, d.s.c. isotherms were analysed only when the instrumental fluctuation did not interfere with the crystallization signal. In these figures, all curves are non-linear (except one cold crystallization line), indicating that a simple Avrami equation does not describe the total isothermal crystallization kinetics sufficiently well. The same observation has been reported in PEEK[7–10], where its crystallization may involve an initial primary crystallization stage and a later secondary crystallization stage. This two-stage crystallization mechanism is also applicable for PEKK. In *Figures 3* and *4*, the estimated Avrami exponent for the initial primary crystallization stage is in the range of 3.5 to 4, and for the later secondary

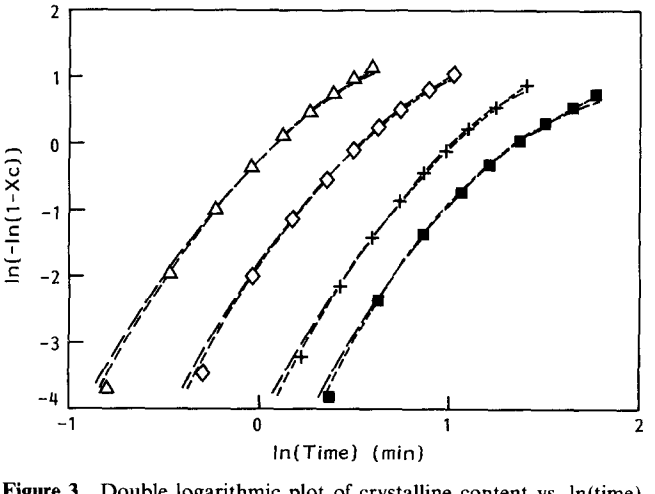


**Figure 3** Double logarithmic plot of crystalline content vs. ln(time) for the melt crystallization measurement of PEKK resin. The short broken curves are the fits using the Hillier model (equation (4)). The long broken curves are the fits using the Velisaris–Seferis model (equation (5)). ■, 310°C; +308°C; ◇, 303°C; △, 298°C

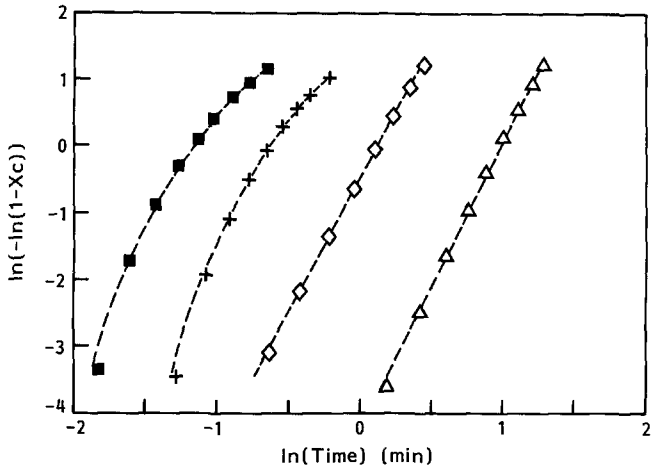


**Figure 4** Double logarithmic plot of crystalline content vs. ln(time) for the cold crystallization measurement of PEKK resin. The broken curves are the fits using equation (4). ■, 221°C; +217°C; ◇, 210°C; △, 200°C

crystallization stage is in the range of 2 to 2.5. These values are again close to those reported for PEEK[8–10].

For three-dimensional athermal nucleation growth, sometimes referred to as instantaneous nucleation growth, i.e. the nucleating density is not a function of time, the value of Avrami exponent is expected[11] to be 3. In the case of thermal conditions, the nucleation becomes sporadic, i.e. the nucleating density depends on both time and temperature, and the Avrami exponent is 4. The latter situation may be close to the initial crystallization stage of PEKK, since the nucleating density is clearly a function of time as observed by the thermal optical analysis. As spherulite impingement occurs, the total crystallization rate decreases significantly. The estimated Avrami exponent for PEKK at this stage ranges from 2 to 2.5, indicating that the nucleation growth becomes lower-dimensional or more diffusion-controlled, or may be a combination of both[12]. Such an argument is consistent with the fact that secondary crystallization usually contains both subsidiary lamellar growth (more diffusion-controlled growth) and isothermal lamellar thickening (lower-dimensional nucleation growth).

We have used the generalized two-stage Hillier equation (equation (4)) to analyse d.s.c. isotherms of PEKK. The Avrami exponent of the primary crystallization $n$ is chosen to be 4 and that of the secondary crystallization $m$ is chosen to be 2. The reason for using 4 for $n$ has been explained before, whereas using 2 for $m$ is somewhat arbitrary. Perhaps, this is because exponent 2 is close to the average value for the three-dimensional diffusion-controlled athermal and thermal nucleation growth, and it also represents some cases of two-dimensional nucleation growth[12]. Hillier has used 1 for $m$, indicating that secondary crystallization within the spherulite obeys a first-order law. This assumption may oversimplify the secondary stage.

Numerical simulation results of the melt crystallization data using equation (4) are summarized in *Table 1*, where the final volume fraction crystallinity of the primary stage ($X_p^0$), both rate constants ($K_p$ and $K_s$) and sums of the squares of standard deviations are listed. In the temperature range of 310 to 298°C, $X_p^0$ is about 0.6 and $X_s^0$ is about 0.4. These values are reasonable considering the following three observations. First, the d.s.c. heating scan of the isothermally melt-crystallized specimens always exhibited two melting peaks. The lower peak temperature was about 10°C above the annealing temperature and the higher one was relatively constant at 340°C; the heat of fusion of the lower peak was about 10% of the total heat of fusion. Bassett *et al.* have indicated that the lower melting peak is only due to the secondary crystallinity[20] (maybe the subsidiary infilling lamellae), and the higher peak may be associated with the primary crystallinity, the residual secondary crystallinity (the lamellar thickening part) and the recrystallized segment. In this case, the value of $X_s^0/X_p^0$ must be larger than 11%. Another observation[15] was that the estimated lamellar thickening factor $\gamma$ for PEKK was about 2.2. The factor $\gamma$ represents the ratio of the final lamellar thickness and the initial lamellar thickness[8]. If we consider that the initial lamellar thickness is due to the primary crystallization[20] and the thickness increase is due to both secondary crystallization and reorganization of the primary crystal, the value of $X_s^0/X_p^0$ must be less than 120%. Finally, we observed[15] that the heat of fusion for a PEKK specimen cooled at 2°C min$^{-1}$ was about 46 J g$^{-1}$ and that at 150°C min$^{-1}$ was about 32 J g$^{-1}$. Both specimens showed no sign of cold crystallization during the heating scan and were fully crystallized. The increase in heat of fusion (14 J g$^{-1}$) between two specimens might be attributed to the additional secondary crystallization of slow cooling. In this case, $X_s^0/X_p^0$ must be larger than 44%, since the heat of fusion for the rapidly cooled specimen (32 J g$^{-1}$) may also contain secondary crystallinity. Therefore, our calculation shows that $X_s^0/X_p^0$ is about 67%, which may be close to the real situation.

We have also used the parallel two-stage Velisaris–Seferis model to analyse the data in *Figure 3*. This model is expressed by the following equation:

$$X_c(t) = X_p^0[1-\exp(-K_p t^n)] + (1-X_p^0)[1-\exp(-K_s t^m)] \quad (5)$$

Numerical results are listed in *Table 2*. We find that

**Table 1** Fit of the generalized Hillier model (equation (4)) using $n=4$ and $m=2$ for melt crystallization of PEKK neat resin (data from *Figure 3*)

| Temperature (°C) | $X_p^0$ | $K_p$ (min$^{-4}$) | $K_s$ (min$^{-2}$) | $SS^a$ |
|---|---|---|---|---|
| 310 | 0.58 | 0.009 | 0.147 | 0.0006 |
| 308 | 0.60 | 0.042 | 0.361 | 0.0007 |
| 303 | 0.65 | 0.273 | 0.973 | 0.0010 |
| 300 | 0.62 | 0.706 | 0.360 | 0.0008 |
| 298 | 0.62 | 1.581 | 3.055 | 0.0005 |

[a] Sum of standard deviations

**Table 2** Fit of the Velisaris–Seferis model (equation (5)) using $n=4$ and $m=2$ for melt crystallization of PEKK neat resin (data from *Figure 3*)

| Temperature (°C) | $X_p^0$ | $K_p$ (min$^{-4}$) | $K_s$ (min$^{-2}$) | $SS^a$ |
|---|---|---|---|---|
| 310 | 0.53 | 0.009 | 0.034 | 0.0025 |
| 308 | 0.71 | 0.024 | 0.058 | 0.0021 |
| 303 | 0.68 | 0.16 | 0.19 | 0.0024 |
| 300 | 0.49 | 0.66 | 0.17 | 0.0017 |
| 298 | 0.69 | 0.93 | 0.52 | 0.0030 |

[a] Sum of standard deviations

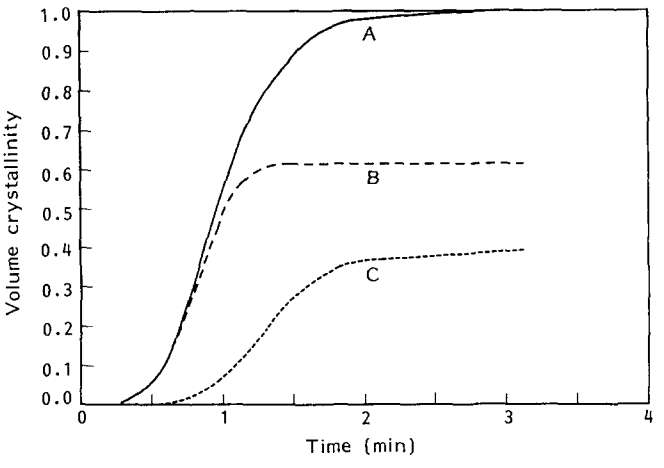


**Figure 5** Isotherm of total volume crystallinity (A) separated into a primary volume crystallinity (B) and a secondary volume crystallinity (C). The data were obtained from the isotherm at 298°C

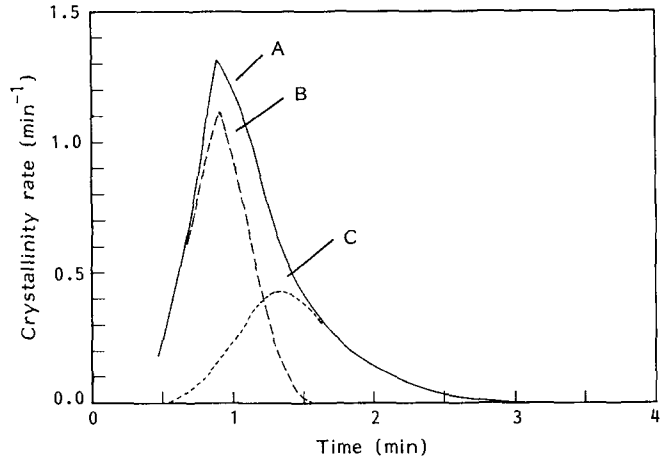


**Figure 6** The time derivatives of *Figure 5*

equation (5) also provides a reasonable fit to the experimental data, although its precision is less than the Hillier model. The Hillier model has an average of standard deviation less than 0.5%, whereas it only has about 3%. The comparison of the fit using equations (4) and (5) is shown in *Figure 3*. We feel that the Hillier model may offer a better physical description of the crystallization kinetics mechanism than the Velisaris–Seferis model. This is because the primary crystallization stage usually occurs before the secondary stage starts, which is closer to the conditions of the Hillier model, rather than at the same time as implied by the Velisaris–Seferis model.

Using the Hillier model, a typical isotherm of PEKK (such as *Figure 1*) can be separated into two distinct crystallization processes, as shown in *Figure 5*. The primary crystallization occurs at the beginning of the crystallization, and the secondary crystallization occurs at a later time. The time derivative of the volume crystallinity of *Figure 5* is shown in *Figure 6*, which resembles d.s.c. crystallization exotherms. In this figure, the peak crystallization time of the total crystallization is very close to that of the primary crystallization. Furthermore, in the primary stage, the peak time is almost equal to the half-time. This suggests that the crystallization peak time vs. temperature plot (*Figure 2*) is equivalent to a half-time of the primary crystallization vs. temperature plot.

Values of the rate constants $K_p$ and $K_s$ directly reflect the crystallization rate of primary and secondary stages, respectively. In *Table 1*, both rate constants decrease with temperature, indicating that the crystallization rates are reduced by lowering the temperature. In the absence of temperature-dependent nucleation rate $N$ and crystal radial growth rate $G$, rate constants $K_p$ and $K_s$ can be interpreted in terms of two- or three-dimensional secondary nucleation processes[13,21]. For a two-dimensional secondary nucleation process, they can be expressed as:

$$K_j = K_j^0 \exp(-\Delta E^*/RT_c) \exp[-C/T_c(\Delta T)] \quad (6)$$

For a three-dimensional process, they can be expressed as:

$$K_j = K_j^0 \exp(-\Delta E^*/RT_c) \exp[-C'/T_c(\Delta T)^2] \quad (7)$$

where $j$ represents p or s, $K_j^0$ is a constant depending on the number of nuclei and $T_c$ is the crystallization temperature. In equations (6) and (7), the first exponential term is associated with the mass transport of crystallizing segments and is expressed by an Arrhenius equation. The apparent Arrhenius activation energy $\Delta E^*$ of amorphous PEKK (above 240°C) is 35–50 kcal mol$^{-1}$, which was estimated by a thermally stimulated current (t.s.c.) method[22]. The second exponential term is associated with the secondary nucleation process, where $\Delta T = T_m^0 - T_c$, $C$ and $C'$ (different units) are constants depending on surface free energies of lamellae, and $T_m^0$ is the equilibrium melting temperature (354°C for PEKK). Equations (6) and (7) can be rearranged as:

$$\ln(K_j) + \Delta E^*/RT_c = \ln(K_j^0) - C/T_c(\Delta T) \quad (8)$$

$$\ln(K_j) + \Delta E^*/RT_c = \ln(K_j^0) - C'/T_c(\Delta T)^2 \quad (9)$$

Thus, by plotting $\ln(K_j) + \Delta E^*/RT_c$ against $1/T_c(\Delta T)$ or $1/T_c(\Delta T)^2$, respectively[21], the mechanism of the secondary nucleation process can be investigated. The least-squares fit of rate $\ln(K_j) + \Delta E^*/RT_c$ vs. $1/T_c(\Delta T)$ or $1/T_c(\Delta T)^2$ are listed in *Table 3*. On the basis of these results, it is not possible to distinguish between a two- or three-dimensional nucleation mechanism since the sum of standard deviations of each fit is very close. The slope of the primary rate constant in *Table 3* can be divided by 3 to approximate the slope determined from the radial growth rate constant. These values are quite reasonable compared with those reported for other polymers such as polypropylene[21] and polyethylene[14]. Furthermore, the slope of the secondary rate constant is smaller than that of the primary rate constant, which indicates the nature of a lower-dimensional nucleation growth.

Numerical simulation results of cold crystallization of PEKK resin using equation (4) are summarized in *Table*

**Table 3** Temperature dependence of rate constants $K_p$ and $K_s$ (from *Table 1*, melt crystallization of PEKK resin) vs. $1/T_c(\Delta T)$ and $1/T_c(\Delta T)^2$ ($\Delta E^*$ was assumed to be 40 kcal mol$^{-1}$)

| | Plot vs. $1/T_c(\Delta T)$ | | Plot vs. $1/T_c(\Delta T)^2$ | |
|---|---|---|---|---|
| | Slope ($K^2$) | $SS^a$ | Slope ($K^3$) | $SS^a$ |
| $\ln(K_p) + \Delta E^*/RT_c$ | $-3.9 \times 10^5$ | 0.992 | $-8.8 \times 10^6$ | 0.993 |
| $\ln(K_s) + \Delta E^*/RT_c$ | $-1.8 \times 10^5$ | 0.681 | $-4.1 \times 10^5$ | 0.680 |

[a] Sum of standard deviations

**Table 4** Fit of the generalized Hillier model (equation (4)) using $n=4$ and $m=2$ for cold crystallization of PEKK neat resin (data from *Figure 4*)

| Temperature (°C) | $X_p^0$ | $K_p$ ($min^{-4}$) | $K_s$ ($min^{-2}$) | $SS^a$ |
|---|---|---|---|---|
| 221 | 0.75 | 163.563 | 31.836 | 0.0012 |
| 219 | 0.79 | 42.369 | 19.018 | 0.0011 |
| 217 | 0.84 | 15.838 | 9.002 | 0.0013 |
| 210 | 0.98 | 0.661 | 1.718 | 0.0012 |
| 200 | 1.04 | 0.020 | 0.801 | 0.0007 |

[a] Sum of standard deviations

**Table 5** Fit of the Velisaris–Seferis model (equation (5)) using $n=4$ and $m=2$ for cold crystallization of PEKK neat resin (data from *Figure 4*)

| Temperature (°C) | $X_p^0$ | $K_p$ ($min^{-4}$) | $K_s$ ($min^{-2}$) | $SS^a$ |
|---|---|---|---|---|
| 221 | 0.75 | 131 | 5.40 | 0.0050 |
| 219 | 0.87 | 35 | 1.80 | 0.0040 |
| 217 | 0.89 | 14.1 | 0.83 | 0.0040 |
| 210 | 0.98 | 0.65 | 0.44 | 0.0018 |
| 200 | 1.05 | 0.02 | 0.42 | 0.0005 |

[a] Sum of standard deviations

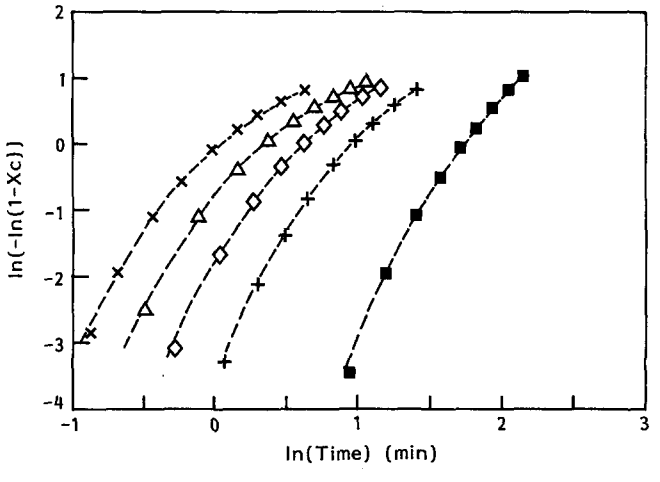


**Figure 7** Double logarithmic plot of relative crystalline content vs. ln(time) for the AS-4/PEKK composite. The broken curves are the fits using equation (4). ■, 314°C; +, 310°C; ◇, 306°C; △, 302°C; ×, 298°C

4, and those using equation (5) are listed in *Table 5*. We found that both models provide similar predictions, but the Hillier model offers a better fit. In *Table 4*, values of $X_p^0$ are very different from those reported for the melt crystallization. Here the value ranges from 0.7 to 1, indicating that the crystallization mechanism is increasingly dominated by the primary crystallization as temperature decreases. This behaviour may be interpreted by the following argument. In the temperature range of 50°C above $T_g$, the molecular mobility is low, which limits the nuclear growth rate by the mass transfer of crystallizing segments. At a sufficiently low temperature, the later-stage secondary crystallization may be significantly reduced, which results in a primary-crystallization-dominant process. The crystallization mechanism between the cold and the melt processes is quite different. The cold crystallization is from the solid glassy state and usually comprises lower molecular mobility and some predetermined crystallizing heterogeneities.

In the case of carbon-fibre-reinforced composite, the isothermal crystallization kinetics of the PEKK matrix is illustrated in *Figure 7*. Again, a two-stage crystallization phenomenon is seen, which is similar to the case of neat resin. Numerical simulation results using equation (4) are listed in *Table 6*. The final primary volume crystallinity $X_p^0$ is also about 60% of the total volume crystallinity. This value is the same as that of the neat resin and is not affected by the presence of fibre. Temperature-dependent rate constants $K_p$ and $K_s$ were also analysed by the two- and three-dimensional nucleation mechanisms. The results are listed in *Table 7*. In this table, the calculated slopes show little difference from those reported in the neat resin (*Table 3*), indicating that the presence of fibre does not affect either crystallization process. This behaviour may be attributed to the fast crystallizing ability of PEKK, as discussed earlier.

## CONCLUSIONS

The crystallization kinetics of PEKK and its carbon-fibre-reinforced composite was analysed by using the generalized Hillier equation for two-stage crystallization. This approach was based on the modified Avrami method, which considered a primary crystallization process at the early stage and a secondary crystallization process at the late stage. The primary crystallization of PEKK was assumed to be three-dimensional, sporadic nucleation growth, with an Avrami exponent of 4; the secondary crystallization was assumed to be diffusion-controlled or two-dimensional nucleation growth, with an Avrami exponent of 2. The numerical fit of the experimental data using this three-parameter model is more precise than the Velisaris–Seferis model. It may also offer a better physical description of the estimated final volume fraction crystallinity for each crystallization

**Table 6** Fit of the generalized Hillier model (equation (4)) using $n=4$ and $m=2$ for melt crystallization of an AS-4/PEKK composite (data from *Figure 7*)

| Temperature (°C) | $X_p^0$ | $K_p$ ($min^{-4}$) | $K_s$ ($min^{-2}$) | $SS^a$ |
|---|---|---|---|---|
| 314 | 0.56 | 0.002 | 0.139 | 0.0008 |
| 312 | 0.54 | 0.011 | 0.176 | 0.0004 |
| 310 | 0.57 | 0.064 | 0.346 | 0.0006 |
| 308 | 0.59 | 0.110 | 0.378 | 0.0009 |
| 306 | 0.59 | 0.268 | 0.518 | 0.0013 |
| 304 | 0.61 | 0.418 | 0.990 | 0.0007 |
| 302 | 0.63 | 0.833 | 0.598 | 0.0028 |
| 300 | 0.63 | 1.520 | 1.309 | 0.0013 |
| 298 | 0.60 | 3.167 | 1.219 | 0.0023 |

[a] Sum of standard deviations

**Table 7** Temperature dependence of rate constants $K_p$ and $K_s$ (from *Table 6*, melt crystallization of AS-4/PEKK composite) vs. $1/T_c(\Delta T)$ and $1/T_c(\Delta T)^2$ ($\Delta E^*$ was assumed to be 40 kcal $mol^{-1}$)

| | Plot vs. $1/T_c(\Delta T)$ | | Plot vs. $1/T_c(\Delta T)^2$ | |
|---|---|---|---|---|
| | Slope ($K^2$) | $SS^a$ | Slope ($K^3$) | $SS^a$ |
| $\ln(K_p)+\Delta E^*/RT_c$ | $-3.7\times10^5$ | 0.982 | $-7.9\times10^6$ | 0.989 |
| $\ln(K_s)+\Delta E^*/RT_c$ | $-1.4\times10^5$ | 0.947 | $-2.9\times10^5$ | 0.947 |

[a] Sum of standard deviations

stage. In the melt crystallization, the final primary volume crystallinity is about 60% (at 298–320°C), which is the same for both the PEKK resin and its carbon-fibre-reinforced composite. In the cold crystallization, the final primary volume crystallinity increases from 70% to 100% as the temperature decreases (from 221 to 200°C), which may be due to the decrease of molecular mobility. Temperature-dependent rate constants for the primary and the secondary crystallization processes were analysed by the two- and three-dimensional nucleation mechanisms. The results did not reveal the type of nucleation growth. The presence of fibre in the composite has little effect on the crystallization rate constant and the relative volume fraction crystallinity for each crystallization stage. The minimal effect of fibre on the total crystallization rate is possibly due to the rapid nucleating ability of PEKK.

## ACKNOWLEDGEMENTS

The authors wish to thank R. Koveleski, T. Genin and J. McKeown for their excellent technical assistance.

## REFERENCES

1 Gardner, K. H. and Matheson, R. R. *J. Polym. Sci. Lett.* 1990, **28**, 243
2 Mijovic, J. *Polym. News* 1989, **14**, 177
3 Jog, J. P. and Kadkarni, V. M. *J. Appl. Polym. Sci.* 1986, **32**, 3317
4 Hartness, T. *J. Thermoplas. Compos. Mater.* 1988, **1**, 210
5 Pratte, J. F., Krueger, W. H. and Chang, I. Y. 34th SAMPE Symp. Proc. 1989
6 Chang, I. Y. *SAMPE Quarterly* 1988, **19**(4), 29
7 Velisaris, C. and Seferis, J. C. *Polym. Eng. Sci.* 1986, **26**(22), 1574
8 Lee, Y. and Porter, R. S. *Macromolecules* 1988, **21**(9), 2770
9 Cebe, P. and Hong, S. D. *Polymer* 1986, **27**, 1183
10 D'amore, A., Kenny, J. M., Nicolais, L. and Tucci, V. *Polym. Eng. Sci.* 1990, **30**(5), 314
11 Blundell, D. J. and Osborn, B. N. *SAMPE Quarterly* 1985, **17**(1), 1
12 Wunderlich, B. 'Macromolecular Physics', Academic Press, New York, 1976, Vol. 2, Ch. 6
13 Hillier, I. H. *J. Polym. Sci.* (*A*) 1965, **3**, 3067
14 Price, F. P. *J. Polym. Sci.* (*A*) 1965, **3**, 3079
15 Chang, I. Y. and Hsiao, B. S. 36th SAMPE Symp. Proc. 1991, in preparation
16 Blundell, D. J. and Osborn, B. S. *Polymer* 1983, **24**, 953
17 Desio, G. P. and Rebenfeld, L. *J. Appl. Polym. Sci.* 1990, **39**, 825
18 Hsiao, B. S. and Chen, E. J. *MRS Symp. Proc.* 1990, **170**, 621
19 Hsiao, B. S. and Chen, E. J. 'Controlled Interphases in Composite Materials' (Ed. H. Ishida), Elsevier, New York, 1990, p. 613
20 Bassett, D. C., Olley, R. H. and Al Rahell, I. A. M. *Polymer* 1988, **29**, 1746
21 Hoshino, S., Meinecke, E., Powers, J. and Stein, R. S. *J. Polym. Sci.* (*A*) 1965, **3**, 3041
22 Sauer, B. B., Avakin, P., Starkweather, H. and Hsiao, B. S. *Macromolecules* 1990, **23**, 5119